4

statoil
Den norske stats oljeselskap a.s

Classification

Requested by

Roald Riise, LET

Subtitle

Co-workers

Jon K. Ringen

Title

Comments to Geco's report: "Special core analysis, well 15/8-1"

STATOIL
EXPLORATION & PRODUCTION
LABORATORY
by
Reidun Furdal

Feb.-84 LAB 83.63

Prepared

20/2-84 Reidun Furdal
Reidun Furdal

Approved

20/2-84 D. Malthe-Sørenssen
D Malthe Sørenssen

Special core analysis were performed by Geco on 10 x 1½" plug samples from well 15/8-1, the Hugin formation. The plug sample material was well fit for doing special core analysis,being well consolidated and homogenous with good porosity and high permeability.
There has earlier been done a special core analysis study by Geco, on the same well, in may 1982. So, it was possible to compare some of the data from these two reports.

1. Routine core analysis.

The routine data show little scatter regarding porosity, while the permeabilities are more spread.
Regression analysis have been used to determine permeability as a function of porosity. The first equation represents the new data, the second equation represents data from both reports.

$\log k = -7.19 + 0.56\emptyset$, $n = 10$, $r^2 = 0.71$
$\log k = -1.94 + 0.25\emptyset$, $n = 25$, $r^2 = 0.40$

As can be observed, the regression coeffisients are poor, one reason is the insufficient spread in porosity.

2. High velocity air flow measurements.

The turbulence factor, β , has been determined for 10 samples.
Refering to Geco's report and the figures on pages 22 to 31 it is seen that a good linear relation has been obtained for x and y in the permeability equation on page 5.
The following empirical equations are given for calculating the turbulence factor.

I $\ln\beta = -1.101\ln K + 23.33$

II $\ln\beta = -1.074\ln (K\cdot\emptyset) + 21.42$

Table 2.1 gives the β -values calculated from these two equations. It is found that by using equation II and thereby relating the turbulence factor to both permeability and porosity, one gets the best agreement between experimental and theoretical data.

Table 2.1 also gives the permeability values for each sample, which can be calculated from the straight line's intercept with the y-axis. A fairly good agreement is achieved between the Klinkenberg corrected permeability and the permeability read from the curves.

Table 2.1.Turbulence factor data.
Experimental and theoretical β -factors.
Experimental permeability and permeability from high flow measurements.

Sample no.	exp. β (cm-1)	eq.I β (cm-1)	eq.II β (cm-1)	K(md)	KL(md)
22.1	$1.43\cdot 10^6$	$0.592\cdot 10^6$	$0.701\cdot 10^6$	418	409
27.1	$1.30\cdot 10^6$	$0.538\cdot 10^6$	$0.647\cdot 10^6$	475	446
30.1	$1.19\cdot 10^6$	$0.864\cdot 10^6$	$0.527\cdot 10^6$*	631	515
35.1	$2.83\cdot 10^6$	$0.117\cdot 10^6$	$0.132\cdot 10^6$	2262	1791
38.1	$8.42\cdot 10^6$	$4.605\cdot 10^6$	$5.50\cdot 10^6$	67.8	63.5
42.1	$6.87\cdot 10^6$	$3.789\cdot 10^6$	$4.18\cdot 10^6$	69.8	75.8
49.1	$5.51\cdot 10^5$	$0.269\cdot 10^6$	$0.308\cdot 10^6$	1058	839
63.1	$2.46\cdot 10^5$	$0.092\cdot 10^6$	$0.109\cdot 10^6$	3049	2210
63.2	$9.76\cdot 10^4$	$0.054\cdot 10^6$	$0.057\cdot 10^6$	4106	3611
77.1	$9.81\cdot 10^7$	$41.40\cdot 10^6$	$46.5\cdot 10^6$	10.9	8.64

3.1 Capillary pressure measurements.

There have been carried out both air/brine and mercury/air capillary pressure measurements on all samples.
Hg-injection data were converted to equivalent air/brine data by the equations:

$$Pc_{Hg} = 5 \cdot Pc_{air}$$

$$Sw = 1 - S_{Hg}$$

It is found a striking deviation in the corresponding Swi values obtained from the two methods.
Like data from previous measurements, Swi from porous plate is higher than Swi from mercury injection.
Regression analysis was used on the air/brine data and the following relation was found between "irreducible" water saturation and permeability:
$Swi = 0.582 - 0.15 \log K$, $r^2 = 0.84$.

Table 3.1.1. "Irreducible" water saturation data.

Sample no.	KL(md)	Swi (frac.) Hg/air data	Swi (frac.) air/brine data
22.1	409	0.10	0.17
27.1	446	0.06	0.14
30.1	515	0.08	0.15
35.1	1791	0.06	0.10
38.1	63.5	0.10	0.23
42.1	75.8	0.09	0.34
49.1	839	0.05	0.15
63.1	2210	0.04	0.14
63.2	3611	0.04	0.12
77.1	8.64	0.18	0.52

3.2 Electrical measurements.

The average saturation exponent, n, was determined to be 1.82 which is equal to the average n in the first report. So, it is recommended to use the value 1.8 for the saturation exponent.

The cementation factors, m, given in this report (I) have been compared to m-values from the former report (II) and a new set of cementation factors, determined from all data available (III).

The actual equations are listed below:

I	$FF = \phi^{-1.7}$	$n = 10$
	$FF = 0.1\phi^{-2.9}$	$n = 10$
II	$FF = \phi^{-1.8}$	$n = 15$
	$FF = 1.5\phi^{-1.6}$	$n = 15$
III	$FF = \phi^{-1.7}$, $r^2 = 0.61$,	$n = 25$
	$FF = 1.1\phi^{-1.7}$, $r^2 = 0.61$,	$n = 25$

It is recommended to use the value 1.7 for the cementation factor and a = 1.

The cation exchange capacity have been determined by two methods, Co/Cw measurements and wet chemistry. To be comparable, the results are here expressed by Q_v $(\frac{meq}{ml})$, and it appears that the two methods do not give the same results. However, based on their practical experience with the two methods, Geco recommends using the data from the Co/Cw measurements. Compared to data in the litterature, these are indicating small amounts of clay present.

Table 3.2.1. Qv-values and a and b in the equation Co = a+bCw

sample no.	a	b	r2	Co/Cw Qv meq/ml	titration Qv meq/ml
22.1	0.01	0.04	0.95	0.07	0.05
27.1	0.01	0.04	1.00	0.07	0.04
30.1	0.01	0.05	1.00	0.05	0.02
35.1	$1.19 \cdot 10^{-4}$	0.05	1.00	0.00	0.03
38.1	0.03	0.04	1.00	0.20	0.03
42.1	0.01	0.04	1.00	0.07	0.02
49.1	0.01	0.05	1.00	0.05	0.01
63.1	0.02	0.06	1.00	0.09	0.02
63.2	0.02	0.06	1.00	0.09	0.02
77.1	0.02	0.03	1.00	0.17	0.07

4. Measurements of overburden conditions.

The measurements of overburden conditions, show no unusual trends. However, one should have chosen the pressure steps with different intervals; there should have been more points between 15 and 200 bar, and more than 7 points in total. This will be corrected by Statoil in future analysis.

5. Relative permeability measurements

5.1 Water permeability

When evaluating the relative permeability data, one started to look at the water permeabilities. These permeabilities have been determined twice, first in connection with the relative permeability measurements, second in connection with the measurements of overburden conditions (see table 5.2.1). There were used two different saturating techniques; In the first case this was saturation by flooding, in the second case, evacuation and saturation under pressure.
Geco says that the degree of saturation obtained by the first method, might not have been 100 %.
It is therefore recommended to use the last data set.

It was also seen that when comparing the Kw/KL values to previous data for the Hugin formation, the second coloumn data gave the best conformity.
When trying to relate the Kw/KL ratio to Klinkenberg permeability, on did not succeed.

Table 5.1.1 The ratio between water permeability and the Klinkenberg corrected permeability.

Sample no.	Kl (md)	Kw I (md)	Kw II (md)	Kw/KL I (md)	Kw/KL II (md)
22.1	409	298	397	0.73	0.97
27.1	446	258	382	0.58	0.86
30.1	515	245	382	0.48	0.74
35.1	1791	980	1702	0.55	0.95
38.1	63.5	51.6	63.8	0.81	1.00
42.1	75.8	27.1	56.0	0.36	0.74
49.1	839	514	714	0.61	0.85
63.1	1577	1066	2195	0.68	1.39
63.2	3611	3833	3997	1.06	1.11
77.1	8.64	6.78	6.663	0.78	0.77

I : $\frac{\overline{Kw}}{KL} = 0.56$ II : $\frac{\overline{Kw}}{KL} = 0.89$

I : saturation by flooding

II : saturation by evacuation and pressure

5.2 Residual gas data

Residual gas measurements have been carried out on ten samples.
First, the gas permeabilities at irreducible water saturation were determined with 20 bar back pressure, to get the approximately Klinkenberg corrected permeabilities.
Obviously, these permeabilities are less than the Klinkenberg permeabilities for dry samples.

However, different permeabilities have been obtained for the same water saturation. Since no systematic deviations are found, it is assumed that this is due to the experimental technique.

The residual gas saturations were determined after water flood and after oil flood, at 4 cc/h and 20 bar back pressure. The following results were obtained:
Residual gas after water flood: 19.9 - 53.0 %
" " " oil " : 35.8 - 54.5 %
These results show that higher residual gas values were obtained from oil flood than from water flood. But, at the same time are the oil permeabilities at residual gas saturation higher than the water permeabilities at residual gas saturation. These two opposite tendencies are probably due to differences in the trapping mechanism.

It was tried to systematize the residual gas data, by using miscellaneous correlations.

By correlating residual gas saturation to permeability one got the following equations:

1. Data from water flood:
   $Sgr = 8.06 + 11.73 \log K$, $r^2 = 0.81$

2. Data from oil flood:
   $Sgr = 37.00 + 4.56 \log K$, $r^2 = 0.47$

It is found that the residual gas saturation is increasing with permeability, and that the water flood data gives the best regression coeffisient.

Sgr was also plotted versus Sgi, and for the oil flood data the tendency was; increasing residual gas saturation with increasing initial gas. The water flood data showed no tendency at all.

The water permeabilities at residual gas were from 4 to 19 % of the water permeability at 100 % saturation. There was not found any correlation between this permeability reduction and Sgr or Kw.

By establishing the ratio Kw(Sgr)/Kg(Swi) there was observed even larger reductions in permeability.

The ratio Ko(Sgr)/Ko(Swi) varied from 0.09 to 0.36, and could not be correlated to, for example, Sgr.

Table 5.2.1. Fluid Properties

All data refer to 20°C and 1 atm

1. Data for formation water

ρ = 1.091 g/cm^3
μ = 1.16 cP

Surface tension for air/water
72.75 mN/m (1)

2. Data for lamp oil:

GECO:	STATOIL:
ρ = 0.752 g/cm^3	ρ = 0.754 g/cm^3
μ = 1.42 cP	μ = 1.43 cP

Surface tension air/oil (STATOIL):
23.1 mN/m

Table 5.2.2 Data from residual gas measurements

SAMPLE NO.	I	IWSGR/IW	IOSGR/IOSW	IRG	IRG-O
22.1	409.0	0.22	0.16	0.12	0.32
27.1	446.0	0.17	0.08	0.10	0.38
30.1	515.0	0.16	0.28	0.25	0.38
35.1	1791.0	0.10	0.10	0.09	0.29
38.1	63.5	0.04	0.13	0.34	0.38
42.1	75.8	0.09	0.17	0.29	0.29
49.1	839.0	0.09	0.10	0.05	0.32
63.1	2210.0	0.09	0.10	0.08	0.30
63.2	3611.0	0.06	0.07	0.05	0.20
77.1	8.6	0.06	0.21	0.69	0.48

SAMPLE NO.	SGI	SGR-W	SGR-O
22.1	0.827	0.377	0.513
27.1	0.860	0.489	0.521
30.1	0.850	0.334	0.545
35.1	0.904	0.406	0.526
38.1	0.766	0.289	0.497
42.1	0.667	0.282	0.455
49.1	0.854	0.434	0.457
63.1	0.865	0.475	0.514
63.2	0.876	0.530	0.483
77.1	0.482	0.199	0.358

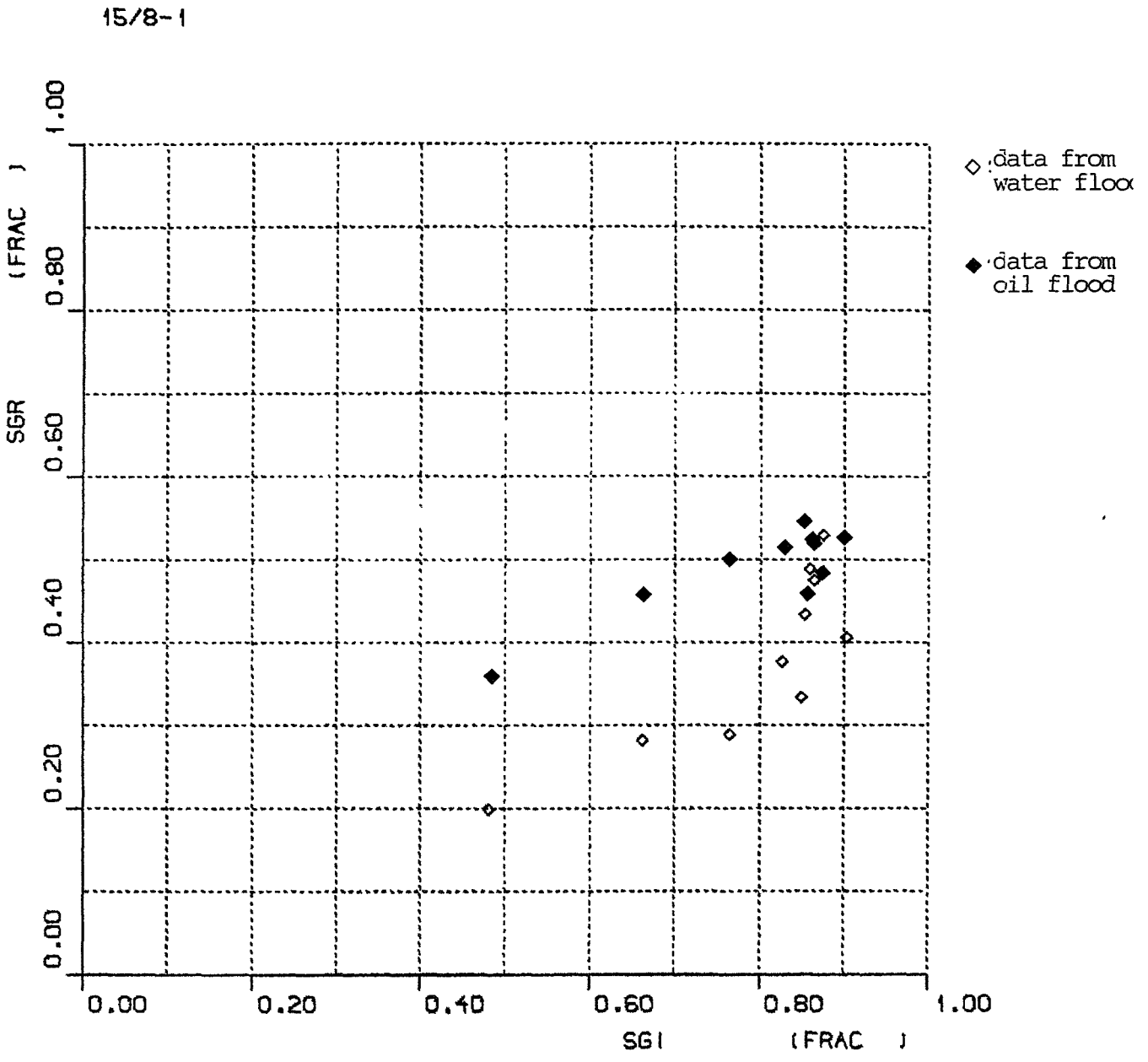

Fig. 5.2.1 Residual gas saturation, Sgr, versus initial gas saturation, Sgi

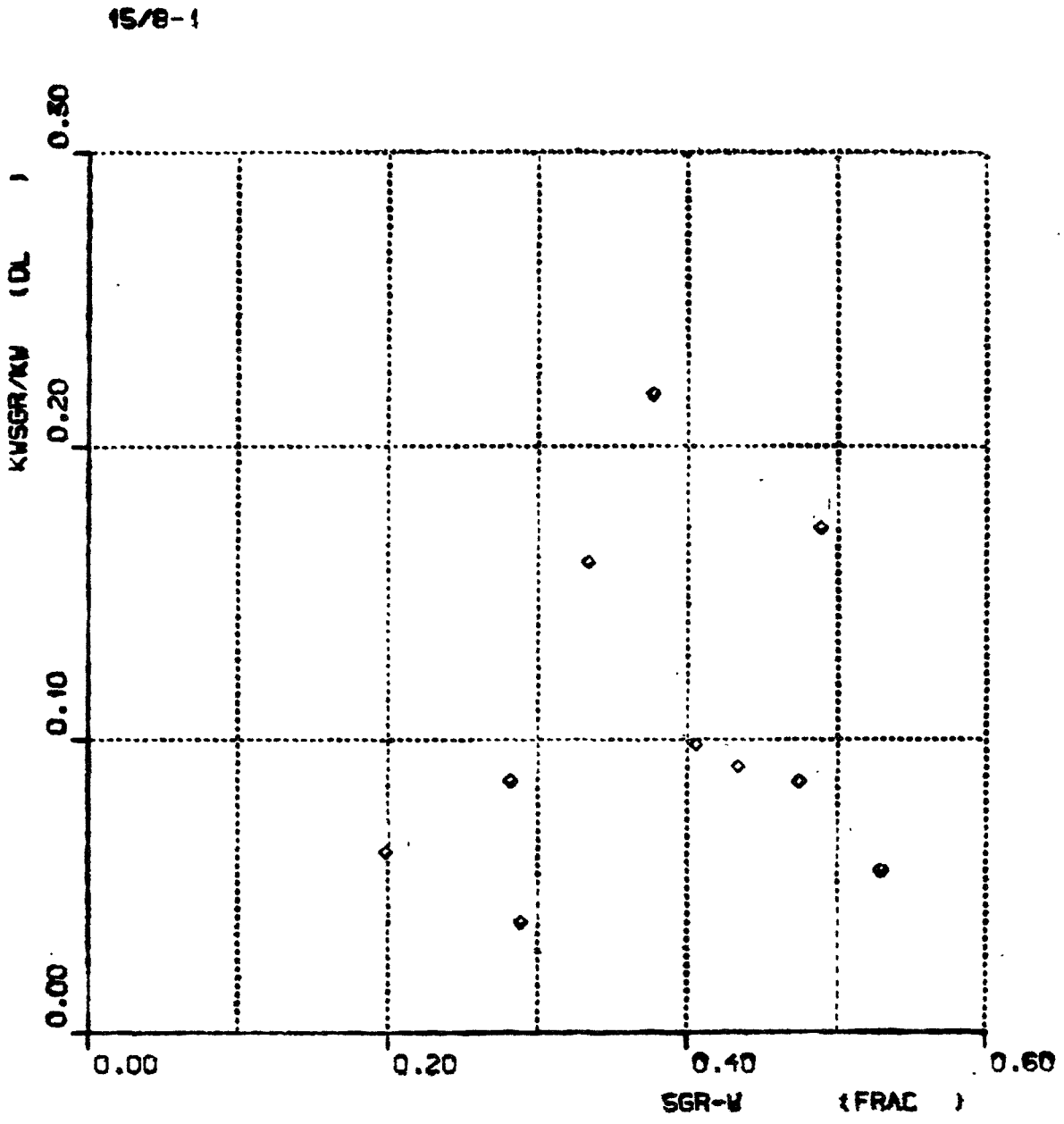

Fig.5.2.2 The ratio KwSgr/Kw versus residual gas after water flood, Sgr-W

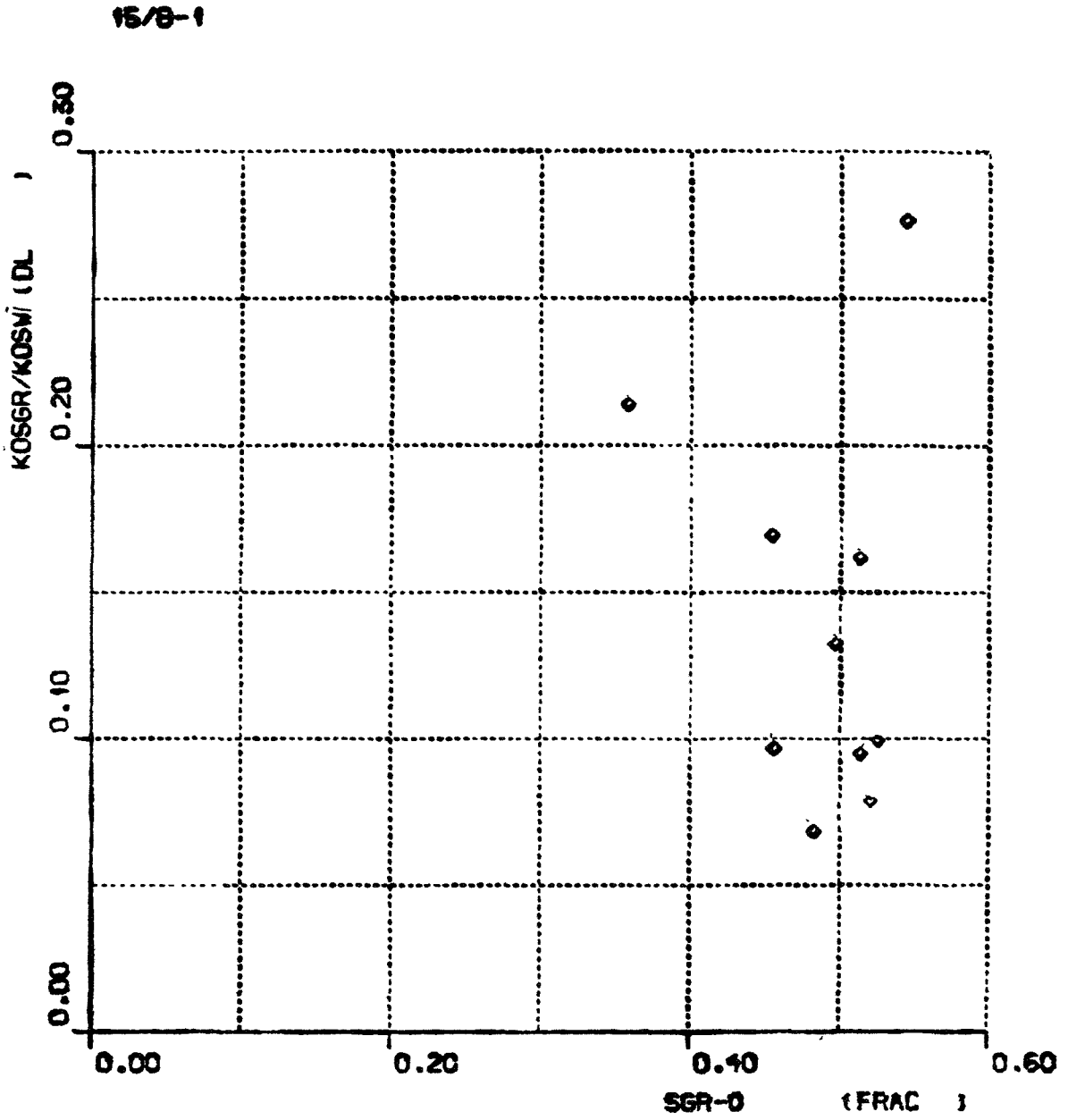

Fig.5.2.3 The ratio KoSgr/KoSwi versus residual gas saturation after oil flood, Sgr-0

5.3. Relative permeability

When performing the relative permeability measurements, the same procedure was used for both the gas-water and the gas-oil system. Shortly, this procedure was "high-rate" gas flood, with 20 bar back pressure. The base permeability was Kg/(Swi).

5.3.1 Gas/water relative permeability curves

The most striking characteristics of the gas/water relative permeability curves, are the very low Krw and Krg values, and the high connate water saturations obtained.

It is therefore suspected that there have been problems with end-effects. The constant differential pressure dp, during the gas-flood was made equal to the dp needed to give a high-rate (400 cc/hr) flow of brine through the sample at Sw = 1.
A comparison of the dp used in the gas-floods with the gas-water capillary pressure curves, shows that for the highest permeability samples, the dp's chosen correspond to points on the first and flat part of the Pc-curves. A contributing factor to the low Krg-endpoints for the high-permeable samples is that they have been flooded with less porevolumes of gas at termination of the experiment. We will recomed that the gas-water relative permeability tests for all samples are repeated at Δp's taken from Pc-tests.

5.3.2 Gas/oil relative permeability curves

The gas/oil relative permeability curves appear to be normal. The Krg and Kro curves for the gas/oil system are all higher than the Krg and Krw for the gas/water system, refering to corresponding gas saturation. The differential pressures used were approximately the same for the two experiments, and it seems that these have been sufficient to get proper drainage of the oil.
One way of explaining this, could be by looking at the fluid properties. As can be seen from table ??, the surface tension for the gas/oil system is approximately 1/3 of the surface tension for the gas/water system. (The value used is for water/air).
The capillary pressure needed to drain the oil should therefore be less than the capillary pressure needed to drain the water, and the problem with end effects has probably not been present.

There is also the expected trend in the data; the Krg curves are spread like a fan, with the high permeability samples showing the lower curves, and the low permeability samples showing the higher curves So, the end point permeabilities were plotted against Klinkenberg permeability and it was observed; decreasing end point permeability with increasing Klinkenberg permeability.

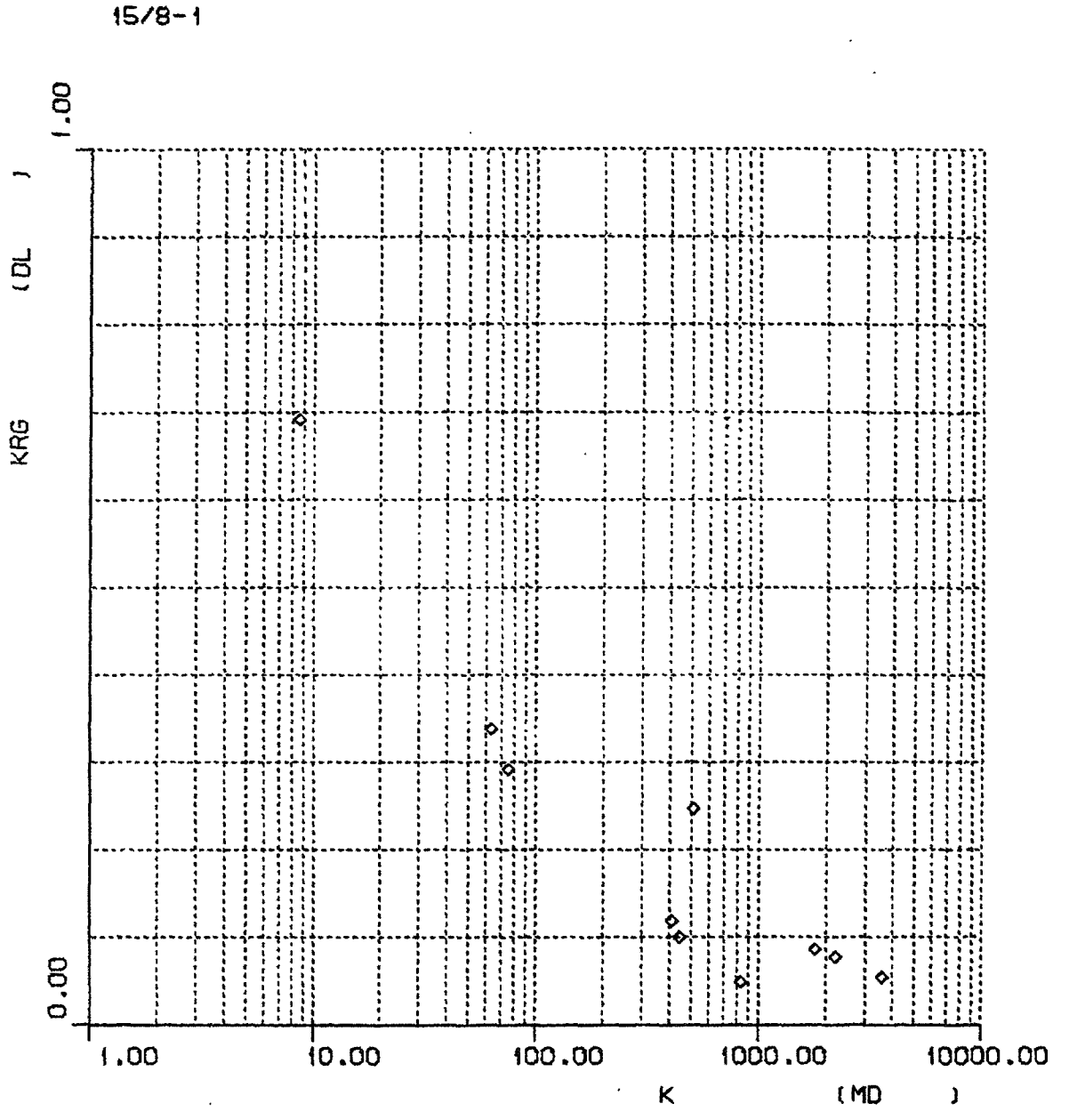

Fig. 5.3.1 End point permeability, Krg (d.l.) from gas/water flood versus Klinkenberg permeability, K(md)

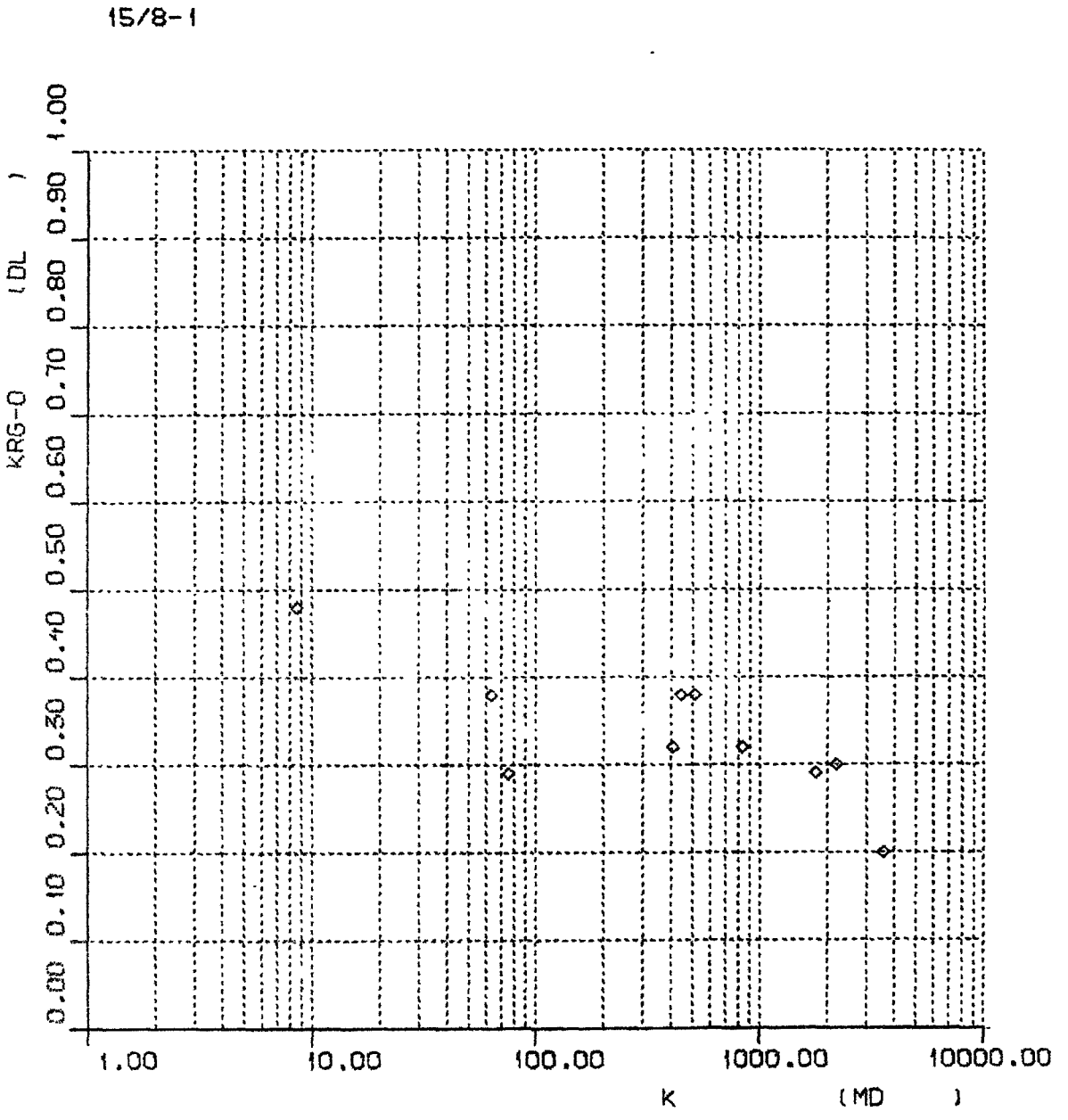

Fig. 5.3.2 End Point permeability from gas/oil flood Krg(d.l.) versus Klinkenberg permeability, K(md)

REFERENCES

1. Robert C. Weast:
"CRC Handbook of Chemistry and Physics"
58th Edition
CRC Press Inc., Florida, 1977-1978